Efficient removal of radioactive waste from solution by two-dimensional activated carbon/Nano hydroxyapatite composites

Nessem El Said* and Amany T. Kassem

Nuclear Fuel Chemistry Hot Labs. And Waste Management Center, Atomic Energy Authority, P.C. 13759, Cairo, Egypt

Abstract. The nano/micro composites with highly porous surface area have attracted of great interest, particularly the synthesis of porous and thin film sheets of high performance. In this paper, an easy method of cost-effective synthesis of thin film ceramic fiber membranes based on Hydroxyapatite, and activated carbon by turned into studied to be applied within the service-facilitated the transport of radioactive waste such as ^{90}Sr, ^{137}Cs and ^{60}Co) as activated product of radioisotopes from ETRR-2 research reactor and dissolved in 3M HNO_3, across a thin flat-sheet supported liquid membrane (TFSSLM). Radionuclides are transported from alkaline pH values. The presence of sodium salts in the aqueous media improves in HNO_3, the lowering of permeability because the initial HNO_3 concentration is improved. The study some parameters on the thin sheet ceramic supported liquid membrane. EDTA as stripping phase concentration, time of extraction and temperature were studied. The study of maximum permeability of radioisotopes for all parameters. The pertraction of a radioactive waste solution from nitrate medium were examined at the optimized conditions. Under the optimum experimental 98.6-99.9% of ^{90}Sr, 79.65-80.3% of ^{137}Cs and ^{60}Co 45.5-55.5% in 90-110 min with were extracted in 10-30 min, respectively. The process of diffusion in liquid membranes is governed by the chemical diffusion process.

Keywords: radionuclides; nHydroxyapatite; nActivated Carbon; thin film supported liquid membrane

1. Introduction

Radioactive wastes from different nuclear facilities have different properties depending on the operations taking place at each facility; wastes are treated according to properties of radioactive types. Radioactive wastes can be classified into several perspectives.

Physical properties of radioactive wastes are in solid, gaseous and liquid form. Radioactive wastes divided into high and low radioactive isotopes. Composition high level waste depends on the composition of spent fuel and the specification of treatment at the reprocessing plant.

The liquid-liquid extraction with supported liquid membrane is one of the first-rate alternate and promising technology for the extraction of metallic ions from solutions over different hydrometallurgical separation processes. The salient functions of the supported liquid membrane (SLM) technique consisting of simultaneous extraction and stripping, low solvent stock, process economic system, excessive performance, much less extractant intake (Efome 2015).

Supported liquid membrane procedure is being carried out for the extraction/separation/removal of precious metal ions from different resources. It is one of the promising technologies for possessing the appealing capabilities along with excessive selectivity and integrate extraction and stripping into one single phase. It's also acts on non-

equilibrium mass-transfer characteristics in which the separation isn't confined via the conditions of equilibrium. The limitations such as aqueous/organic phase ratio, emulsification, flooding and loading limits, phase disengagement, huge solvent inventory, and so forth, can be avoided (Wu *et al*. 2016). The supported liquid membranes (SLM) have applications in each industrial and analytical field for separation, pre-concentration, and treatment of waste water (Park *et al*. 2015). Accordingly, SLM technology has been taken into consideration as an attractive opportunity over traditional unit operations for separation and concentration of metal ions within the hydrometallurgical method (Dong *et al*. 2016, Woo *et al*. 2016, Izatt *et al*. 1989).

This new and economic approach to manufacture resistant porous membrane supports consists of Nano hydroxyapatite which includes $(CaCO_3)/AC/\beta$-Tricalcium phosphate. The porous mullite based ceramics had been acquired by solid, stable reaction response. One-of-a-kind calcite quantities (10-28 wt%) had been introduced into activated carbon/β-Tri calcium phosphate if you want to manage pores forming with appropriate distribution and sizes. Based on a pore distribution and formed phases, a Nano hydroxyapatite+15 wt% calcite (K15C) mixture changed into decided on for flat sheet supported liquid membrane configurations. A porosity of 60-72% (Kasai *et al*. 2008, Ghadiri *et al*. 2017, Sobieski *et al*. 2017).

Carrier-mediated transport through supported liquid membranes is currently diagnosed as a probably precious era for selective separation and concentration of toxic and precious metal ions. The fundamental components

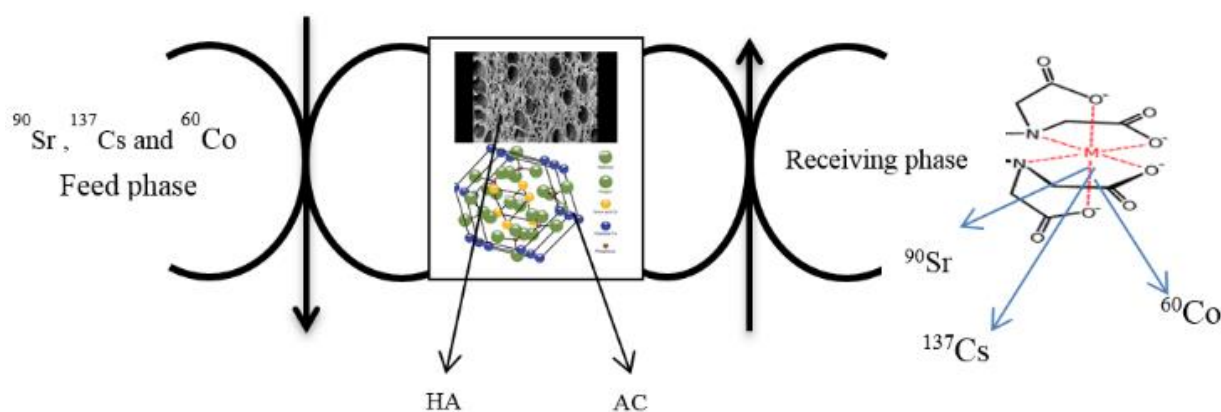*Corresponding author, Professor
E-mail: nesnaelsaid@yahoo.com

Fig. 1 Transport mechanism of the metal ions across the supported liquid membrane (SLM) (Banjjar *et al*. 2012)

concerning metal ion transport and the influencing factors are surveyed in terms of information modeling, membrane performance (permeability, selectivity, stability) (Wódzki *et al*. 1995, El-Said *et al*. 2014).

Removal of radioactive contaminants plays a vital role in maintaining the surroundings and the disposal of waste via the drinking water treatment processes. They took a look at the fact that this work is limited to removal from waste and get better all the factors of ^{137}Cs, ^{90}Sr and ^{60}Co. They are fission products with a high fission yield. The focus will be on the aqueous radioactive waste manipulate includes treatment, shipping, storage, and disposal of the wastes, further to environmental monitoring of radionuclide releases. The choice of disposal approach depends upon the waste type. In widely recognized, wastes are remoted till the radionuclides which consist of ^{137}Cs, ^{90}Sr and ^{60}Co had been removed to the amount of approximately 95 %, 56 % and 53 % respectively on one complete waft of the liquid waste via the filter column. After 12 hr such entire circulations, approximately 80% of ^{134,137}Cs were eliminated from the liquid waste, but the further removal of ^{60}Co and ^{90}Sr grow to be not placed. Separation of radioactive isotopes for ^{60}Co, ^{90}Sr and ^{137}Cs within the nitrate medium with the useful resource of using Hydroxyapatite Ceramic supported membrane (Kislik *et al*. 1996, Danesi *et al*. 1981, Danesi *et al*. 1987, Christensen *et al*. 1978, Gopi *et al*. 2017).

The article is to display a method and chemical route for the preparation of nano and micro ceramic materials to the removal of radioactive waste ^{137}Cs, ^{90}Sr and ^{60}Co from nitrate, aqueous media through a thin sheet, ceramic liquid membrane using the two composites nano hydroxyapatite/Activated carbon as carrier is investigated. The aim was to optimize various operational parameters, and thus obtain efficient removal radioactive waste from supported liquid membranes.

2. Experimental

2.1 Reagents and materials

The extractant nano-hydroxyapatite/Activated carbon was used as supplied by the nature bone from animal and palm fronds. Other chemicals used were AR (analytical reagent) grade, radioactive metals from ^{137}Cs, ^{90}Sr and ^{60}Co in nitrate media solutions were prepared by dissolving in deionized water. The different concentrations used in the experiments were prepared from a stock solution of 2.5×10^{-3} M in radioactive waste. The pH of the solution was adjusted by addition of NaOH solutions. During the experiments, the pH was continuously controlled using pH-meter of the type B-417 HANNA instrument. In nitrate media, the radioactive solutions were prepared in a similar manner using $HM[NO_3]^{-2}$.

2.2 Transport of metals (n) ions through thin flat sheet supported liquid membrane (TFSSLM)

The transport of radioactive metals from the feed phase to the strip phase by thin film supported liquid membrane in this studied system is a coupled counter current transport. By this mechanism $Mn+$ and $H+$ move by diffusion in opposite direction through the membrane by the carrier RH (Wojciech *et al*. 2017, Kolev *et al*. 1997, Kool 1987). The transportation of the radioactive ions in particular from the feed phase to the EDTA as stripping phase where both the phases are separated by liquid membrane supported with the relevant carrier acting as the barrier is as demonstrated in the Fig. 1 (Kumar *et al*. 2005).

Atomic Absorption/Emission Spectrophotometer /210/VGP (AAS), buck scientific, U.S.A., though in experiments, the metal concentrations in the stripping phase were also analyzed to verify active metal transport. The radioactive metals concentration in the aqueous solution was found to be reproducible in ±1%. The effective permeability coefficients, P*, have been determined from the concentration with time where the time-dependent concentration in the aqueous phase and converted right into a feature, k, also depending on the initial analytical (general) concentration in phase A and the volumes of both the aqueous levels. The logarithm of this function modification linearly with time, t, after a steady- K_{ext} nearly 100 shown the equation (1) (Nawaz *et al*. 2015, Gherrou *et al*. 2002, Cheng *et al*. 2015).

$$K_{ext}=[C]_t/[C]_0= -A/V \, Pt \qquad (1)$$

where V is the volume of the feed phase solution, A is the

effective membrane area, $[C]_0$ and $[C]_t$ are the concentrations of metal in the feed phase at zero time and at decline time. That the above expression was obtained under condition of the fully intermix in the feed phase.

3. Results and discussion

3.1 Effect of nitric acid on the Radionuclides' transport

In the pH variety of 2.5 to 5.5, the extraction of radionuclides nitrate with the aid of thin layer supported liquid membrane is represented via the overall equilibrium (Wafa *et al*. 2014). That is pH-impartial and where in aqueous and organic denote species in two levels, respectively. L represents the active substance of the extractant. On this response, M^+ represents a cation, consisting of ^{137}Cs ,^{90}Sr or ^{60}Co respectively.

That is pH-impartial and where in aqueous and organic denote species in two levels, respectively. L represents the active substance of the extractant. On this response, M^+ represents a cation, consisting of ^{137}Cs, ^{90}Sr or ^{60}Co respectively. The value of the extraction steady and calculate (K_{ext}) for the above equilibrium and reached into over 96.87.

$$H^+{}_{aq}Sr(OH)_2(NO)_3{}^- + \overline{2L} + HSr(OH)_2(NO)_3{}^-\overline{L_2} \quad (2)$$
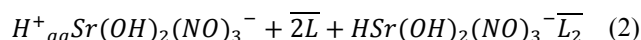
3.2 Effect of stirring speeds on the feed and stripping phases

The transport in all experiments, stirring speeds of 1300-1700 rpm were used for the feed and stripping phases, respectively. In the preceding experiments, accomplished with a feed phase containing 2.5×10^{-5} M ^{137}Cs ,^{90}Sr or ^{60}Co respectively at pH 2.5-5.5, stripping phase of EDTA and a membrane phase of 0.052 M nano HA+AC in chloroform (blended isomers, it need to be noted here that at some phase in all of the work, the chloroform is used to explain this aggregate), showed that the permeability coefficient will become without a doubt impartial (2.5×10^{-3} cm/s) of the stirring velocity in these ranges, which additionally indicates that a minimal value of the thickness of the feed phase thin film is reached (Sobieki *et al*. 2017).

3.3 Effect of permeability coefficient on radioisotopes

Effect of permeability coefficient on radionuclides show that in Fig. 2 depicts that the effects obtained for the transport of different radioactive waste in nitrate media in the Table 1: Presence of sodium salts. The organic phase used within the experiments contained membrane composite (0.01 M) in chloroform. The aqueous phase contained 5×10^{-3} M of radionuclides at pH 2.5-5.5. If it is taken into consideration that once no salts were added to the feed phase the permeability coefficient become 9×10^{-6} cm/s, 6.9×10^{-6} and 3×10^{-6} for ^{137}Cs ,^{90}Sr or ^{60}Co respectively. Consequences shown in Table 1 show that the presence of the inorganic sodium nitrate salts in the feed phase increases the transport of radionuclide's with little have an effect on of the counter anion of the salt on the permeability coefficient.

Table 1 Effect of the permeability coefficient in presence of different salts on radionuclides {^{137}Cs, ^{90}Sr and ^{60}Co} transport

^{90}Sr nanocomposites membrane(M)	$P \times 10^{-6}$ (cm/s)
5×10^{-2}	0.035
4.5×10^{-2}	3.08
2.5×10^{-2}	3.12
^{137}Cs	$P \times 10^{-6}$ (cm/s)
5×10^{-2}	0.024
4.5×10^{-2}	2.21
2.5×10^{-2}	2.30
^{60}Co	$P \times 10^{-6}$ (cm/s)
5×10^{-2}	0.016
4.5×10^{-2}	1.49
2.5×10^{-2}	1.59

Table 2 Effect of different extractant on ^{137}Cs, ^{90}Sr or ^{60}Co respectively

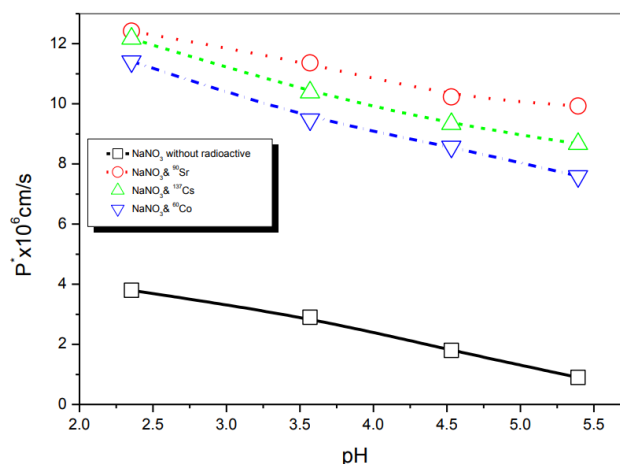| ^{90}Sr Salt	$P \times 10^{-6}$ (cm/s)
NaNO₃	9
NaCl	5.43
Na₂SO₄	3.87
^{137}Cs	$P \times 10^{3}$ (cm/s)
NaNO₃	6.9
NaCl	4.21
Na₂SO₄	2.77
^{60}Co	$P \times 10^{3}$ (cm/s)
NaNO₃	3
NaCl	1.98
Na₂SO₄	1.05

Fig. 2 Effect of permeation coefficient for different radionuclides on the feed phase concentration

To have a look at the effect of the presence of nitrate salts in the feed phase on radionuclides permeation in extra element, a hard and fast of experiments was done at a regular NaNO₃ concentration of 3M and ranging pH values. In Fig. 2 the version of the ^{137}Cs ,^{90}Sr or ^{60}Co permeation coefficient is plotted vs aqueous pH of the feed phase for the transport of Cs(NO₃)⁻, Sr(NO₃)⁻² and Co(NO₃)⁻² respectively, from aqueous solutions containing 5×10^{-2} for ^{137}Cs ,^{90}Sr or ^{60}Co. The organic phases contained 0.05 M Nano HA+AC/chloroform in it is able to be noted that in

the absence of NaNO$_3$, the transport of ^{137}Cs ,^{90}Sr or ^{60}Co has a tendency to decrease because the pH will increase; whereas inside the presence of NaNO$_3$, the transport is higher at all pH values, and remains nearly steady. This effect need to be due to the attributable that the transport occurs via solvation of ion pairs Na$^+$Cs(NO$_3$)$^-$, Na$^+$Sr (NO$_3$)$^-_2$ and Na$^+$Co(NO$_3$)$^{-2}$ by using the organic reagent. The quantity ratio of membrane solution was 1:1. Concentration of membrane as 0.01 M. The proportion of ^{90}Sr approximately 97.7%, while ^{137}Cs about 78.5% and ^{60}Co approximately 55.5%. Test the search in the provision of chemicals and results in addition to increase the value of extraction when selecting pH ~5.5 as an occurrence within the most reliable pH so while we discovered out this extraction: ^{90}Sr > ^{137}Cs > ^{60}Co respectively.

3.4 Effect of extractant solutions on radionuclides transport

In Table 2, the received ^{137}Cs ,^{90}Sr or ^{60}Co permeation coefficients, at distinct concentrations of nano composites membrane in the chloroform as organic phase, are given as a way to observe the effect of extractant concentrations variant on ^{137}Cs, ^{90}Sr or ^{60}Co transport. Experiments were performed at a steady pH value of 2.5-5.5. Aqueous levels contained 2.5x10^{-2} M radionuclides and 3M NaNO$_3$. Within the natural phase, exceptional extractant concentrations in chloroform had been used. Outcomes received revealed no big change in the steel permeability at higher service concentrations. The constant permeation coefficient value or restricting permeability (P$_{lim}$), in equation (3) can be attributed to the assumption that diffusion inside the membrane is negligible as compared with the aqueous diffusion and the permeation process is managed via the diffusion inside the stagnant film of the feed phase consequently:

$$P_{\lim} = \frac{D_{aq}}{d_{aq}} = 9x10^{-6}\,cm/s \qquad (3)$$

Assuming a value of 9x10^{-6} cm^2/s for Daq (average diffusion coefficient) (Juang 2004), then daq = 7.3x10^{-6} cm. This value (daq) is the minimal thickness of the stagnant aqueous diffusion layer in the present experimental conditions.

3.5 Effect of the carrier concentration on permeability of radionuclides

The results concerning transport of ^{137}Cs, ^{90}Sr or ^{60}Co from a feed phase containing 8x10^{-6} M in 0.5 M HNO$_3$, Fig. 3 shown that the stripping phase being EDTA, and varying concentrations of nano composites/Chloroform in the variety 0.13 to 0.72 M dissolved in chloroform, revealed no trade within the permeation coefficient (2.5x10^{-3} cm/s) at higher carrier concentrations (0.1-0.9 M) towards the value of 2.9x10^{-6} cm/s obtained for a 0.22 M nanocomposites solution in chloroform. For this reason, to Eq. (3) and thinking about the value of 4x10^{-3} cm/s as the proscribing coefficient permeability value, the thickness of the aqueous diffusion thin film is calculated as 2.8x10^{-3} cm.

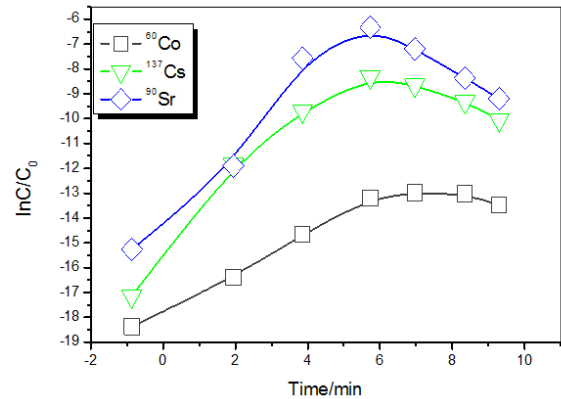Fig. 3 Effect of the carrier concentration on permeability of ^{90}Sr, ^{137}Cs and ^{60}Co: 0.5 mg/L, Feed acidity: 3M NaNO$_3$+0.1M HNO$_3$: 0.5M EDTA as stripping solution
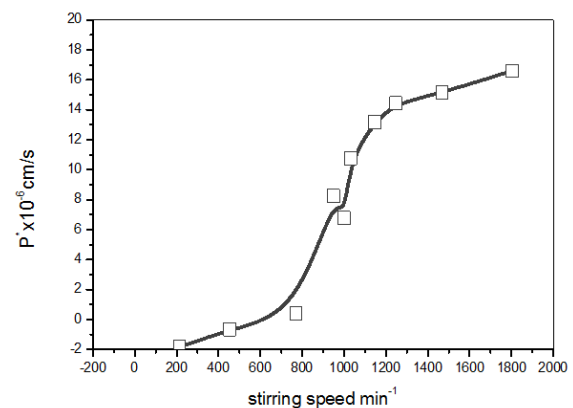

Fig. 4 Effect of stirring speed in the feed phase

Moreover, influent COD concentration in MBRs was consistently maintained as 500 mg/L. Average effluent concentration of COD in C-MBR was 98.2 ± 0.2 whereas with the addition of QQ embedded CEBs in QQ-MBRs, the effluent concentration of COD was 98 ± 0.1 (Table 2). Thereby, no adverse effects of QQ on the organic removal efficiency was observed (Surwade et al. 2015, Safarpour et al. 2015).

3.6 Effect of the stirring speed within the feed phase

Experiments have been performed to establish adequate hydrodynamic conditions. The permeability of the membrane become studied as a function of the stirring speed at the feed phase solution facet as preceding tests had proven that the version of the stirring speed at the receiving solution facet had little effect on radionuclides transport. Effects received are proven in Fig. 4. Effect of stirring speed in the feed solution near consistent permeability for stirring speeds higher than 1300 rpm/ min^{-1} become obtained. Therefore, the thickness of the aqueous diffusion layer and the aqueous resistance to mass transfer had been minimized. The diffusion contribution of the aqueous species to the mass transport system is thought to be constant. Stirring speeds of 1900 rpm/ min-1 and 800 rpm/ min-1 were maintained throughout all the experiment for the stripping and the feed phase respectively.

Table 3 Effect of initial radioactive metals concentration on radioactive nuclides permeability and metal flux

M	^{90}Sr	P$\times 10^{-6}$ (cm/s)
0.29		5.4
1.25		6.2
2.87		6.8
	^{137}Cs	
0.29		1.78
1.25		2.84
2.87		3.2
	^{60}Co	
0.29		0.016
1.25		1.49
2.87		1.59

Table 4 Selectivity of the radionuclides in HNO$_3$

Metal	P* (cm/s)	$\beta_{radioactive/M}$
^{90}Sr	3.9x10^{-3}	15.46
^{137}Cs	2.9x10^{-3}	19.13
^{60}Co	1.8x10^{-3}	22.54

3.7 Effect of the initial radioisotopes concentration

From different contents of radioactive ions are of experiments becomes accomplished the use of feed solutions with nitric acid and sodium nitrate, which permeability various from 6.8x10^{-6} to a 3.2x10^{-6} and 2.88x10^{-6} M for ^{90}Sr, ^{137}Cs and ^{60}Co respectively, in 0.5 M HNO$_3$. The organic phase contained 0.50 M nano composites as thin sheet ceramic supported liquid membrane in chloroform. Table 3 shows the variant of radionuclide's permeation coefficient and flux for one-of-a-kind ^{137}Cs, ^{90}Sr or ^{60}Co concentrations. This displays that the increase of the preliminary ^{137}Cs, ^{90}Sr or ^{60}Co concentration elevated the preliminary metal flux (Kouki *et al.* 2014)

3.8 Effect of separation factor and permeability coefficient of radioactive ions from aqueous solution

Given that base metals are generally determined in the ^{137}Cs, ^{90}Sr and ^{60}Co in nitric media bearing solutions, the selectivity of the existing transport machine towards the presence of various metals in the feed phase was investigated by means of using a membrane phase of 0.5 M nHAP/AC in chloroform, and the feed phase containing 3.9x10^{-3}, 2.9x10^{-3} and 1.8 x10^{-3} M for ^{137}Cs, ^{90}Sr and ^{60}Co respectively, 1M HNO$_3$ from the outcomes received (Table 4), it is miles inferred that radionuclides changed into ideally transported over those base metals. The selectivity with appreciate to ^{90}Sr seems to be enough to separate this radioactive metals selectively from the bottom metals; it can be additionally referred to here that within the present experimental conditions, the permeation coefficient for ^{90}Sr is not tormented by the presence of other metals within the solution (5.88x10^{-3} cm/s while only ^{90}Sr is present in the feed solution in opposition to the value given in Table 4), hence, in the present system the crowding effect seems now not to persuade the transport of ^{90}Sr.

3.9 Models of the diffusional parameters

Special models were proposed for flat-sheet supported liquid membrane transport, between them, modellization proposed within the literature (Castillo *et al.* 2002, Harruddin *et al.* 2017) were and still is successfully implemented to some of systems due to the fact the experimental conditions usually hired permit quality utility of the equations (Alguacil 2004, Van de Voorder 2004, Bukhar *et al.* 2004, Uheida 2004, Yang 2000, He 2000, Wang 2004, Juang 2004 and Geist *et al.* 2000). In the present investigation, the mass switch of MR$^+$ throughout the membrane is defined thinking about diffusion parameters. It's far assumed that the resistance of interfacial reaction to the general transport is negligible in flat-sheet supported liquid membranes (Wang *et al.* 2000, Juang 2004). Accordingly, the interfacial flux due to the chemical response has no longer been considered as the chemical reactions taking location on the aqueous feed segment-membrane (and membrane-receiving solution) interfaces are fast (Noble *et al.* 1987), and it is counseled that speedy chemical reactions can be taken into consideration to occur instantaneously relative to the diffusion processes (Lin *et al.* 2001). The sort of simplified sort of information evaluation is used in the present paintings; this is fairly valid due to the extraordinarily thick membrane guide used in this research (Juang 2004). Accordingly to the version derived, the mass transfer of MR+ taken into consideration the diffusion of the metal via the aqueous feed boundary layer, the reversible chemical reaction on the interface and the diffusion of the metallic-extractant complicated species in the membrane. The extraction equilibrium of MR$^+$ by way of nHAP/AC dissolved in chloroform may be described by means of the reaction shown in Eq. (4) and can be expressed of the extraction constant (K$_{ext}$) as Eq. (4).

$$k_{ext} = \frac{[MR^+(NO_3)^{-2}.L]_{org}}{[MR^+(NO_3)^{-2}]_{org}[L]^3_{org}} \quad (4)$$

The MR$^+$ transport rate for radionuclides are decided by means of the rate of diffusion of MR$^+$-containing species through the feed phase diffusion layer and the rate of diffusion of MR$^+$-nHAP/AC species through the membrane. Then, the flux of MR$^+$-crossing the membrane may be derived through applying Fick's first diffusion regulation to the diffusion layer at the feed phase side and to the membrane. The permeability coefficient (P) of the membrane was calculated according to the following equation (5):

$$P^* = KV_{0 \to a} / A\varepsilon \quad (5)$$

where V$_{0-a}$ is the volume of the initial and final concentration of feed solution, A is the area of the membrane film and ε is the membrane porosity.

$$P = \frac{k_{ext}[L]^3_{org}}{V_0 + V_a k_{ext}[L]^3_{org}} \quad (5\text{-}1)$$

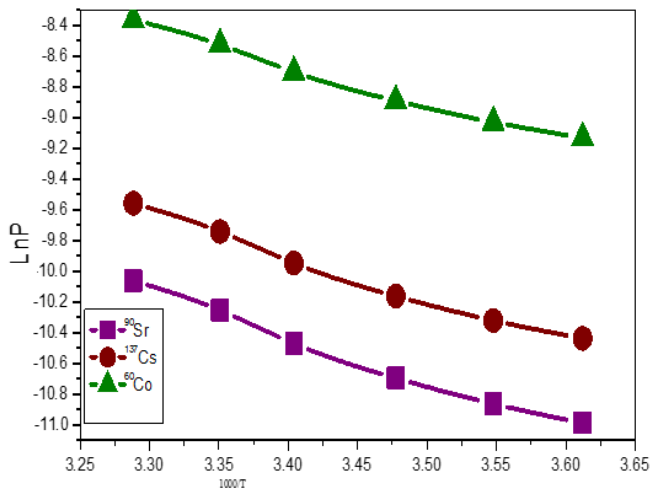P* (permeability coefficient) via plotting 1/P* as a

Fig. 5 Plot of LnP against t, min for effect of temperature on the radioactive isotopes = 0.05M NaNO₃, HA- AC = P5/chloroform

Fig. 6 Plot the relation between decontamination behaviors against permeability coefficient

characteristic of $1/K_m$ $[L]_{org}$ for various extractant concentrations in chloroform. There are three diffusional processes in a ceramic system are affected to a different degree by a high number of factors, such as carrier, organic, solvent and ceramic supported membrane, so find, different solutions through the membrane may be approximated by the diffusion through a ceramic membrane flat sheet. The individual mass transfer coefficient k_m may be expressed as (Vakifahmetoglu 2011).

$$K_m = \frac{\varepsilon D_m}{\tau^2 R_i \ln R_0 / R_i} \qquad (6)$$

where τ is the membrane tortuosity and ε is the membrane porosity. D = corresponding parameters where D = ε/τ and D as void space, R_0/R_i denoting hydraulic radius of obstacles. Table 4 shows the selectivity of the radionuclides in 3M HNO₃. In the case of the ⁹⁰Sr, ¹³⁷Cs or ⁶⁰Co-nano composites membrane gadget, the following equations supply the reactions and extraction constants of the corresponding extraction equilibria at 3M HNO₃ in the aqueous phase: Table 4. The diffusion coefficient of the ⁹⁰Sr, ¹³⁷Cs or ⁶⁰Co complex in the bulk organic phase can be expected from the diffusivity within the membrane via the following expression.

The following equations supply the reactions and extraction constants of the corresponding extraction equilibria at 3M HNO₃ in the aqueous phase:

$$H_{aq}^+ + MR^+ NO_3^{2-} + L_{org} \Leftrightarrow H^+ MR^+ NO_3^{2-}.L_{org} \quad (7)$$

Dm gives a decrease value than that of the bulk diffusion coefficient; this is on account of diffusional resistance due to the micro- porous membrane positioned between the feed and stripping phases.

3.1.1 Effect of temperature
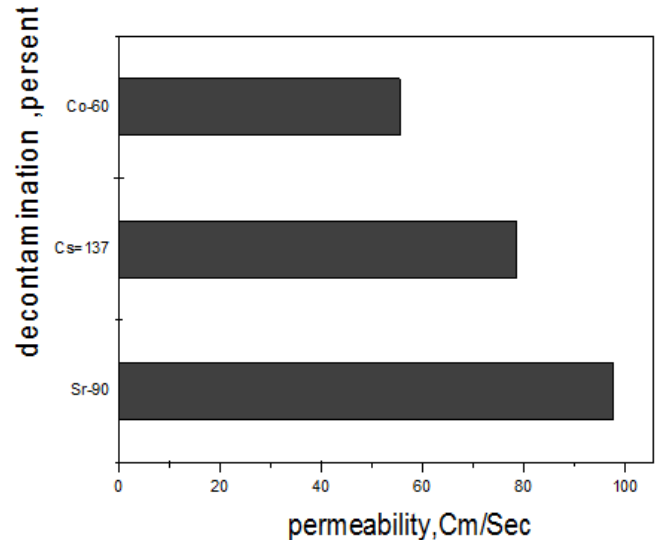Increase in the permeability coefficient with increasing

temperature as much as 298 k. At constant stirring rate (Fig. 5), prediction model for separation of radioactive waste. The natural logarithm of the rate constant became determined to be linear with recognizing to 1/T which allowed estimating the activation energy of the slope of the straight line in keeping with the Arrhenius and Eyring equations. The range of activation energies from temperature 278-298 K for the studied system was calculated to be 15.45, 18.523 and 12, k cal/mol at our hydrodynamic conditions for ⁹⁰Sr, ¹³⁷Cs and ⁶⁰Co respectively.

3.1.2 Optimization of Cs(I), Sr(II) and Co(II) removal from aqueous solution
The effect of membrane solvents on strontium and cesium transport from nuclear fuel reprocessing concentrate solutions to demineralized water through a thin sheet-supported liquid membrane has been studied using nanocomposites impregnated in polymer poly[N-methyl-β -alanine]-b-(N-benzyl-β-alanine)]P5, /chloroform. Studied the highest values of the distribution coefficients of strontium and cesium were obtained from nitrated medium as membrane solvents, the permeability's of strontium and cesium were determined only when a membrane solvent was used for which stable thin sheet supported liquid membrane (TSSLM) were obtained. Separation Factor (SF) of strontium and cesium calculated and found to increase at higher radiation dose and suggested the possibility of getting better decontamination on prolonged use the thin film supported liquid membrane system. Fig. 6 shows the relation between the permeability and decontamination behavior of all metal ions. From Fig. 6 it is obvious that as the permeability increases from 9x10⁻⁶, 7x10⁻⁶ and 3x10⁻⁶ Cm/Sec for ⁹⁰Sr, ¹³⁷Cs and ⁶⁰Co respectively. The decontamination uptake efficiency increases from 10⁻¹, 10⁻⁴, 10⁻⁶. From the above mentioned discussion, we can conclude the permeability of ⁹⁰Sr > ¹³⁷Cs > ⁶⁰Co since the decontamination efficiency increase.

4. Conclusion

Two dimensional of n- activated carbon-n Hydroxyapatite impregnated in polymer poly[N-methyl-β-alanine]-b-(N-benzyl-β-alanine)]P5, formed flat sheet ceramic supported liquid membrane. On this painting at the FSSLM, deals with the overall principles, observed with the aid of the transportation and characterization of supported membrane considered the quality alternate of separation radioactive waste relies upon on a few parameters.

• Determine the pH on feed phase dissolved radioactive in 3M HNO$_3$ +0.1 M NaNO$_3$ at pH = 4.9. The extraction of ^{90}Sr ~97.7%, ^{137}Cs ~78.5% and ^{60}Co ~55.5%.

• The parameter of permeability coefficient as increase with increasing concentrations of feed phase, which effect of concentration of diffusion layer increase, and because of lower of nitric acid attention at pH ~2.5-5.5. The maximum of permeability 9x 10^{-6} ,7x 10^{-6} and 3x 10^{-6} Cm/Sec for ^{90}Sr, ^{137}Cs and ^{60}Co respectively.

• And examine of the extraction equilibrium depends at the shipping of radionuclides thru disc supported membrane and calculated values from mass balance for the proposed version to prove that the numerical treatment of ^{90}Sr > ^{137}Cs > ^{60}Co respectively.

• The depicts of the transport of radioactive waste from feed solution attention 3.5x10^{-5} M and decide the thickness of disc ceramic membrane in aqueous diffusion layer and show the experimental situations. The most permeability 18x10^{-3}, 8.5x10^{-3} and 5x10^{-3} M for ^{90}Sr, ^{137}Cs and ^{60}Co respectively.

• Study of the decontamination behavior against the permeability coefficient, as the optimum conditions the permeability increased and the decontamination decreased.

• Stripping phase in the carrier phase as accelerated from 0.5-0.95 M for HNO$_3$ and NaNO$_3$, the richness element accelerated 2.5 into 5. The concentration of nitric acid, growing because of decreased the stripping phases and create the opposition between negatively charged ions due to reducing stripping phase so that the most permeability became determined to be (13, 11, 6) x 10-6 cm/Sec for ^{90}Sr, ^{137}Cs and ^{60}Co, respectively.

• Sooner or later, temperature increase because of growth the permeability coefficient. The activation energies from temperature range 278-298 K for the studied gadget became calculated to be 15.45, 18.5 and 23.12, kcal/mol at our hydrodynamic situations which show the reaction follow a ramification method. The increase within the permeability coefficient with growing temperature as much as 298 K. At constant stirring rate, the natural logarithm of the value constant was located to be linear with appreciate to hydrodynamic conditions and the prediction model for separation of radioactive waste.

• Finally, the main benefit of this work is the usage of natural bone substances from the environment reasonably in the paintings of a ceramic membrane flat sheet able to withdraw the radioactive metal ions that pollute the environment through the solution to exist.

References

Alguacil, F.J. and Alonso, M. (2004), "Transport of Au(CN)2- across a supported liquid membrane using mixtures of amine Primene JMT and phosphine oxide Cyanex 923", *J. Hydrometallurgy*, **74**(1-2), 157-163.

Bukhar, N., Chaudry, M.A. and Mazhar, M. (2004), "Cobalt(II) transport through triethanolamine-cyclohexanone supported liquid membrane", *J. Membr. Sci.*, **234**(1-2), 157-165.

Castillo, E., Granados, M. and Cortina, J.L. (2002), "Liquid-supported membranes in chromium (VI) optical sensing: Transport modelling", *Analytica Chimica Acta*, **464**(2), 197-208.

Christensen, J.J., Lamb, J.D., Izatt, S.R., Starr, S.E., Weed, G.C., Astin, M.S., Slitt, B.D and Izatt, R.M. (1978), "Effect of anion type on rate of facilitated transport of cations across liquid membranes via neutral macrocyclic carriers", *J. Am. Chem. Soc.*, **100**(10), 3219-3220.

Danesi, P.R. Reichley-Vinger, L. and Rickert, P.G. (1987), "Lifetime of supported liquid membranes: The influence of interfacial properties, chemical composition and water transport on the long-term stabilities of the membranes", *J. Membr. Sci.* **31**(2-3), 117-145.

Danesi, P.R., Horwitz, E.P., Vandegrift, G.F. and Chiarizia, R. (1981), "Mass transfer rate through liquid membranes: Interfacial chemical reactions and diffusion as simultaneous permeability controlling factors", *Sep. Sci. Technol.*, **16**(2), 201-211.

Dong, G., Hou, J., Wang, J., Zhang, Y., Chen, V. and Liu, J. (2016), "Enhanced CO2/N2 separation by porous reduced graphene oxide/Pebax mixed matrix membranes", *J. Membr. Sci.*, **520**, 860- 868.

Efome, J.E., Baghbanzadeh, M., Rana, D., Matsuura, T. and Lan, C.Q. (2015), "Effects of super hydrophobic SiO2 nanoparticles on the performance of PVDF flat sheet membranes for vacuum membrane distillation", *Desalination,* **373**, 47-57.

El-said, N., Ali, M.M.S. and Hamd, M.M. (2014), "Nanoapatite for Nanotechnology: Part (III) A novel process for the fabrication and Improvement of nanoporous apatites from synthetic hydroxyapatite (HAp) in vitro activated carbon", **7**(1), 2278-5736.

Geist, A., Plucinski, P. and Nitsch, W. (2000), "Mass transfer kinetics of reactive multi-cation coextraction to bis (2-ethylhexyl) phosphoric acid", *Solvent Extr. Ion Exch.*, **18**(3), 493-515.

Ghadiri, M., Marjani, A. and Shirazian, S. (2017), "Development of a mechanistic model for prediction of CO$_2$ capture from gas mixtures by amine solutions in porous membranes", *J. Environ. Sci. Pollut. Res.*, **24**(16), 236.

Gopi, D., Ramya, S., Rajeswari, D., Surendiran, M. and Kavitha, L. (2014), "Development of strontium and magnesium substituted porous hydroxyapatite/poly (3, 4-ethylenedioxythiophene) coating on surgical grade stainless steel and its bioactivity on osteoblast cells", *Colloids Surf. B: Biointerfaces*, **114**, 234-240.

Harruddin, N., Saufi, S.M., Faizal, C.K.M., Mohammad, A.W., and Ming, H.N. (2017), "Supported liquid membrane using hybrid polyether sulfone/graphene flat sheet membrane for acetic acid removal", *J. Phys. Sci.*, **28**, 111.

He, D.S., Ma, M. and Zham, Z. (2000), "Transport of cadmium ions through a liquid membrane containing amine extractants as carriers", *J. Membr. Sci.*, **169**(1), 53-59.

Izatt, R.M., Roper, D.K., Bruening, R.L and Lamb, J.D. (1989), "Macrocycle-mediated cation transport using hollow fiber supported liquid membranes", *J. Membr. Sci.*, **45**(1-2), 73-84.

Juang, R.S., Kao, H.C. and Wu, W.H. (2004), "Analysis of liquid membrane extraction of binary Zn(II) and Cd(II) from chloride media with Aliquat 336 based on thermodynamic equilibrium models", *J. Membr. Sci.*, **228**(2), 169-177.

Kasai, A., Willershausen, B., Reichert, C., Röhrig, B., Smeets, R. and Schmidt, M. (2008), "Ability of nanocrystalline hydroxyapatite paste to promote human ligament cell

proliferation", *J. Oral Sci.*, **50**(3), 279-285.

Kislik, V.S. and Eyal, A.M. (1996), "Hybrid liquid membrane (HLM) system in separation technologies", *J. Membr. Sci.*, **111**(2), 259-272.

Kolev, S.D., Argiropoulos, G., Cattrall, R.W., Hamilton, I.C. and Paimin, R. (1997), "Mathematical modelling of membrane extraction of gold (III) from hydrochloric acid solutions", *J. Membr. Sci.*, **137**(1-2), 261-269.

Kool, J.B., Parker, J.C. and Van Genuchten, M.T. (1987), "Parameter estimation for unsaturated flow and transport models — A review", *J. Hydrology*, **91**(3-4), 255-293.

Kouki, N., Tayeb, R. and Dhahbi, M. (2014), "A flat-sheet supported liquid membrane based on Aliquat® 336 as carrier for the removal of salicylic acid from aqueous solution", *Desalination Water Treat.*, **52**(25-27), 4745-4754.

Kumar, A. Haddad, R., Alguacil, F. J. and Sastre, A.M. (2005), "Comparative performance of non-dispersive solvent extraction using a single module and the integrated membrane process with two hollow fiber contactors", *J. Membr. Sci.*, **248**(1-2), 1-14.

Lin, S.H. and Juang, R.S. (2001), "Mass-transfer in hollow-fiber modules for extraction and back-extraction of copper (II) with LIX64N carriers", *J. Membr. Sci.*, **188**(2), 251-262

Nawaz, R., Ali, K. and Arshad, M. (2015), "Recovery of mercury using a trioctylphosphine oxide-based supported liquid membrane system", Environ. Eng. Sci., **32**(11), 948-959.

Noble, R.D. and Way, J.D. (1987), "Liquid membrane technology: An overview", *Liquid Membranes: Theory and Applications*, American Chemical Society, Washington, DC, U.S.A.

Park, M., Phuntsho, S., He, T., Nisola, G., Tijing, L., Li, X., Chen, G,. Chung, W. and Shon, H. (2015), "Graphene oxide incorporated polysulfide substrate for the fabrication of flat-sheet thin-film composite forward osmosis membranes", *J. Membr. Sci.*, **493**, 496-507.

Safarpour, M., Khataee, A. and Vatanpour, V. (2015), "Effect of reduced graphene oxide/TiO2 nanocomposite with different molar ratios on the performance of PVDF ultrafiltration membranes", *J. Sep. Purif. Technol.*, **140**, 32-42 .

Sobieski, W. and Lipinski, S. (2017), "The analysis of the relations between porosity and tortuosity in granular beds", *J. Technical Sci.*, 85.

Uheida, A., Zhang, Y. and Muhammed, M. (2004), "Transport of palladium (II) through hollow fiber supported liquid membrane facilitated by nonylthiourea", *J. Membr. Sci.*, **241**(2), 289-295.

Vakifahmetoglu, C. (2011), "Fabrication and properties of ceramic 1D nanostructures from preceramic polymers: A review", *Adv. Appl. Ceramics: Struct., Funct. Bioceramics.*, **110**(4),188-204.

Van de Voorde, I., Pinoy, L. and de Ketelaere, R.F. (2004), "Recovery of nickel ions by supported liquid membrana (SLM) extraction", *J. Membr. Sci.*, **234**(1-2), 11-21.

Wang, L., Paimin, R., Cattrall, R.W., Shen, W. and Kolev, S.D. (2000), "The extraction of cadmium (II) and copper (II) from hydrochloric acid solutions using an Aliquat 336/PVC membrane", *J. Membr. Sci.*, **176**(1), 105-111.

Wódzki, R. and Sionkowski, G. (1995), "Recovery and concentration of metal ions. II Multimembrane hybrid system", *Sep. Sci. Technol.*, **30**(13), 2763-2778.

Woo, Y.C., Tijing, L., Shim, W.G., Choi, J.S., Kim, S.H., Drioli, E. and Shon, H.K. (2016), "Water desalination using graphene-enhanced electrospun nano fiber membrane via air gap membrane distillation", *J. Membr. Sci.*, **520**, 99-110.

Wu, X., Zhao, B., Wang, L., Zhang, Z., Zhang, H., Zhao, X. and Guo, X. (2016), "Hydrophobic PVDF/graphene hybrid membrane for CO2 absorption in membrane contactor", *J. Membr. Sci.*, **520**, 120-129.

Yang, C.F. and Cussler, E.L. (2000), "Reactive dependent extraction of copper and nickel using hollow fibers", *J. Membr. Sci.*, **166**(2), 229-238.

ED